Journal of Energy Storage 44 (2021) 103367

Contents lists available at ScienceDirect

Journal of Energy Storage

journal homepage: www.elsevier.com/locate/est

Experimental investigation on heat transfer and air flow behavior of latent heat storage unit in a facade integrated ventilation system

Tugce Pekdogan [a,*], Ayça Tokuç [b], Mehmet Akif Ezan [c], Tahsin Başaran [a]

[a] Department of Architecture, Izmir Institute of Technology, Izmir, Turkey
[b] Department of Architecture, Dokuz Eylul University, Izmir, Turkey
[c] Department of Mechanical Engineering, Dokuz Eylul University, Izmir, Turkey

ARTICLE INFO

Keywords:
Mechanical ventilation
Latent heat
Decentralized ventilation systems
Facade integrated systems
Staggered tube bundle

ABSTRACT

All-air central HVAC systems are widely applied to provide fresh and conditioned air, which is very important for users to lead healthy and productive lives. Decentralized systems are another mechanical solution to ensure indoor air quality and thermal comfort with a heat recovery ventilation system integrated into the building wall. These commercially available systems store sensible energy in the heat exchanger. In this study, an experimental real-size staggered tube bundled prototype with phase change material (PCM), which stores latent thermal energy, was proposed/designed and full-scale experiments were carried out in laboratory conditions. The experimental setup includes two spaces that simulate indoor and outdoor conditions that are separated by an insulated aerated concrete wall. In the prototype, two ducts embedded in the wall contain staggered tube bundles filled with PCM, which are positioned perpendicular to the airflow to recover heat for supply and exhaust ventilation modes. The thermal performance of this prototype is investigated for different operating times, namely, 15, 20, and 30 min. The average air energy change of the latent heat recovery ventilation system values is between 20 and 35 kJ approximately for the operating times. The supply mode efficiency result is an average of 50% and exhaust mode efficiency is 25%.

1. Introduction

Today, people spend more than 90% of their time indoors either in the office or at home [1]. Therefore, buildings should be designed not only to provide adequate accommodation but also to create a healthier environment. This study examines the relationship between air quality, human health, and energy use. Such studies have increased recently in light of the COVID-19 pandemic, which has raised concerns about indoor air quality (IAQ) [2]. In an attempt to slow or stop the transmission of the virus, scientists and government officials have focused on implementing infectious disease prevention measures such as asking people to stay at home. Such recommendations have led to an increased interest in ensuring IAQ and related mechanical ventilation systems. On the other hand, since the building sector consumes more energy than the industry and transportation sectors [3], many studies focus on the effect of building energy use on the environment and methods to reduce this energy use. In response to environmental concerns, many countries have implemented compulsory measures to decrease energy consumption while maintaining thermal comfort. The most common measures include properly insulating the building envelope and reducing infiltration loads [4]. However, this creates airtight buildings that are not well-ventilated, and lead to decreased IAQ. Both natural and mechanical ventilation methods can help provide fresh air inside the buildings. For natural ventilation, the pressure difference between the indoor and outdoor environment is the driving force. However, if the wind-driven ventilation and stack effect are insufficient or cannot be controlled, mechanical ventilation systems are preferred. The differences between mechanical and natural ventilation in terms of indoor air pollutants were compared, occupants living in mechanically ventilated houses had a higher health status and their health was significantly improved [5]. The results from healthcare units' IAQ indicate that adequate control of CO_2 concentration and relative humidity balance effectively reduces the risk of infection through the air with the use of mechanical ventilation systems [6]. When the air quality in schools was investigated by ventilation rates, the concentrations of pollutants in low-energy school buildings were lower than those that were naturally ventilated [7]. Comparing mechanically ventilated buildings with naturally ventilated buildings can provide a better understanding of the IAQ of buildings because different ventilation systems can have different effects on

* Corresponding author.
E-mail address: tugcepekdogan@iyte.edu.tr (T. Pekdogan).

https://doi.org/10.1016/j.est.2021.103367
Received 1 July 2021; Received in revised form 27 September 2021; Accepted 1 October 2021
Available online 11 October 2021

Nomenclature

c_p	specific heat capacity (J/kg·K)
h_{sf}	latent heat of fusion (J/kg)
$\dot{m}$	mass flow rate (kg/s)
η	efficiency
Q	thermal energy (J)
T	temperature (℃)
t	time (s, min)
ΔT	temperature difference (℃)
Δt	time difference (s)

Abbreviation

AHU	air handling unit
CVS	centralized ventilation system
DVS	decentralized ventilation system
HRV	heat recovery ventilation
HVAC	heating, ventilation, and air conditioning
IAQ	indoor air quality
LHTES	latent heat thermal energy storage
PCM	phase change material

Subscript

in	inlet
int	initial
out	outlet

indoor particle concentrations. Considering IAQ conditions, mechanical ventilation can reduce indoor particle concentrations in residential buildings [8]. Also, some publications have discussed and examined mechanical ventilation systems' energy use potential in different climates [9,10]. Advanced designs of new buildings are beginning to have mechanical systems that bring outdoor air into the indoor environment. Some of these designs include energy-efficient heat recovery ventilators to improve IAQ [1]. Heat recovery ventilation (HRV) systems ensure the efficient use of energy by transferring heat from the exhaust air to the fresh air supply [11]. There are various methods to recover heat from exhaust air for mechanical system applications [12], and these systems typically recover 60–95% of the energy in the exhaust air thereby significantly improving buildings' energy performance [13]. Although there are several studies on heat recovery systems, shortcomings remain in the research and development of using recovery systems in building applications and also the use of wall integrated systems [14].

Considering heat recovery effectiveness, energy consumptions are limited [9] and decentralized ventilation systems (DVSs) have lower pressure losses [10] when DVSs and centralized ventilation systems (CVSs) are compared. Also, the large volume requirements of a CVS [15] can be avoided by using a DVS and embedding HRV systems into the building wall. HRV systems that store sensible heat are commercially available. However, wall integrated HRV systems can only meet the fresh air requirement of relatively small spaces by using multiple units because of the low capacity of their sensible heat energy storage units and small fans. These wall integrated HRV systems usually involve electronically driven two-way fans. The indoor air that is expelled to the outdoors flows through a ceramic material and transfers its thermal energy to the ceramic block, and the temperature variations within the ceramic block correspond to the sensible heat storage. After completing the expelling process, the fan works in the opposite direction, transferring fresh outdoor air to the indoors. Removable filters in the system control the outdoor contaminants and the two units running simultaneously prevent indoor pressure imbalances.

The commercially available wall-integrated DVSs generally consist of an air supply grill, an air filter, an axial fan, and a ceramic heat exchanger, from outdoors to indoors. These products can provide different fresh air flow rates depending on their fan capacities and the selected control levels. The fans usually work in one direction for 70 s. The number and placement of units inside a space depend on the size of the space to be ventilated, the desired air change rate, and the homogeneous fresh air distribution. In addition to considering esthetic value in architectural designs, DVSs are easier to control and generate less noise than CVSs. However, the proper design, selection, and implementation of energy-efficient ventilation systems require a holistic approach to the buildings and users. According to ASHRAE [16], air to air energy recovery equipment for the room-based DVS that is installed in the exterior walls, sensible effectiveness is typically in the range of 80–90%. Furthermore, in the previous work of the authors executed the same experimental setup but differently by using a sensible heat recovery ventilation system included a ceramic heat exchanger [17] and found that the supply efficiency for simulated summer conditions, when the unit is operated for 7.5 min, is up to 89% and for 10 min, the exhaust efficiency is decreased to 45%.

Beside sensible heat storage, latent heat recovery is possible in condensing conditions (i.e., heating mode). For the latent effectiveness, the manufacturers report that desiccant treated fixed-bed regenerators are in the 60% to 80% range [16]. Thus, latent heat thermal energy storage (LHTES) is frequently used today in the heating and cooling sector due to its energy-saving and high efficiency [18,19]. Therefore, heat recovery DVSs can achieve higher thermal energy storage capacities by using latent heat in addition to sensible heat. The narrow temperature ranges and system designs associated with PCM in LHTES have attracted the attention of many researchers [20–25].

Providing comfortable thermal conditions while using less energy by adding PCMs to the building elements has a wide range of applications. Soares et al. [20] examined how and where PCMs are used in LHTES systems and explored the relationship between building solutions and the building's energy performance. They concluded that LHTES systems with PCM can contribute to increase indoor thermal comfort and system efficiency, reduce the heating and cooling peak loads, and reduce energy consumption. Thus, to maximize the system's benefits, the phase change temperature, type of PCM, and the amount of material must be determined accurately. Some mechanical systems store latent heat in heat recovery ventilation, in addition to the studies. Experimentally and numerically designed and fabricated studies include a real-size heat exchanger unit with PCM [21] integrated into a ventilated window [22] or staggered tubes [19]. These studies were conducted to improve IAQ, performed experimental and numerical simulations to determine the most suitable design criteria by changing the heat exchanger forms, the amount of PCM, and properties of the PCM.

As seen in the previous articles, a wide variety of energy-efficient systems have been developed and evaluated for the recovery of waste heat energy from buildings. In many studies, the performance of DVSs was compared with CVSs under different climatic conditions and the findings show that DVSs cause lower pressure losses and provide more energy savings. Several studies [11,17,23,24] mentioned wall integrated HRV systems, a new concept (especially for DVS), and evaluated their potential applications for residential ventilation. Thus, by using PCM, more thermal energy storage capacity can be provided in a more compact geometry than the sensible heat thermal energy storage solution. Based on the studies compiled above, and to the best of our knowledge, there are no numerical and experimental studies into the energy and flow analysis of a decentralized wall integrated HRV system with PCM. Thus, this current study proposes such a unit design and experimentally evaluates its thermal performance and air flow behavior. In the current study, firstly, a full-scale experimental system is built up that includes a new HRV prototype. This prototype is characterized thermally under controlled conditions. The fan performance and the heat recovery unit performance are calculated according to calibrated and measured data. Thus, how different operational cycle periods affect the energy consumption by the HRV prototype is investigated. Lastly,

the results are analyzed and the conclusions on the performance are given.

2. Experimental setup and procedure

2.1. Experimental setup

The full-scale experiments were carried out in the Building Physics Laboratory of the Faculty of Architecture, Izmir Institute of Technology. An experimental chamber, previously used for the thermal study of a double-skin facade [25–28], was redesigned and prepared for this study. The experimental setup includes two spaces that simulate indoor and outdoor temperature conditions. They are separated by an insulated aerated concrete wall. Parametric studies have been carried out to determine the performance of two wall integrated HRV systems with tube bundled prototypes containing PCM.

The experimental setup shown in Fig. 1 consists of eight main parts: The aerated concrete wall (I) separates the simulated indoor (II) and outdoor (III) environments. The dimensions of the simulated indoor environment (II) are 2.7 m depth, 1.5 m width, and 3 m height, and it has 10 cm thick insulated panel walls. The simulated outdoor environment (III) has measurements of 2 m depth, 1.5 m width, and 3 m height. The experimental HRV systems (IV) are mounted inside the two air ducts (V), which are positioned outside of the wall for being accessible while taking measurements inside the units and the ducts insulated against heat transfer. The heating/cooling constant temperature bath (VI) with a flowmeter condition the indoor (II), while a cooling group (VII) and a thermostat-controlled heater (VIII) condition the outdoor (III) environment. The heating/cooling systems use wall-hung serpentines to condition the air as shown in Fig. 1. Thermocouples (shown as *T*) continuously measure temperatures from the points shown schematically in Fig. 1.

The experimental decentralized ventilation unit with heat recovery (IV in Fig. 1) uses a heat exchanger to transmit heat from the exhaust air to the supply air and can be installed directly on a facade. Fig. 2 shows the overview of the ventilation system with a tube bundle prototype, which consists of covers for inside (1) and for outside (2), filter (3), fan (4), and the tube bundle heat exchanger unit (5). The air taken from outside passes through the filter before it reaches the indoor

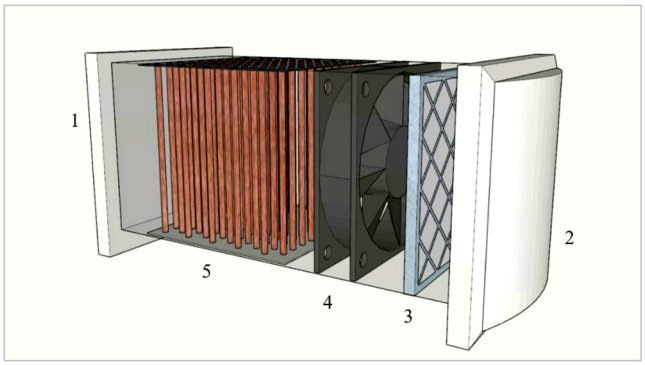

Fig. 2. The experimental heat recovery system overview.

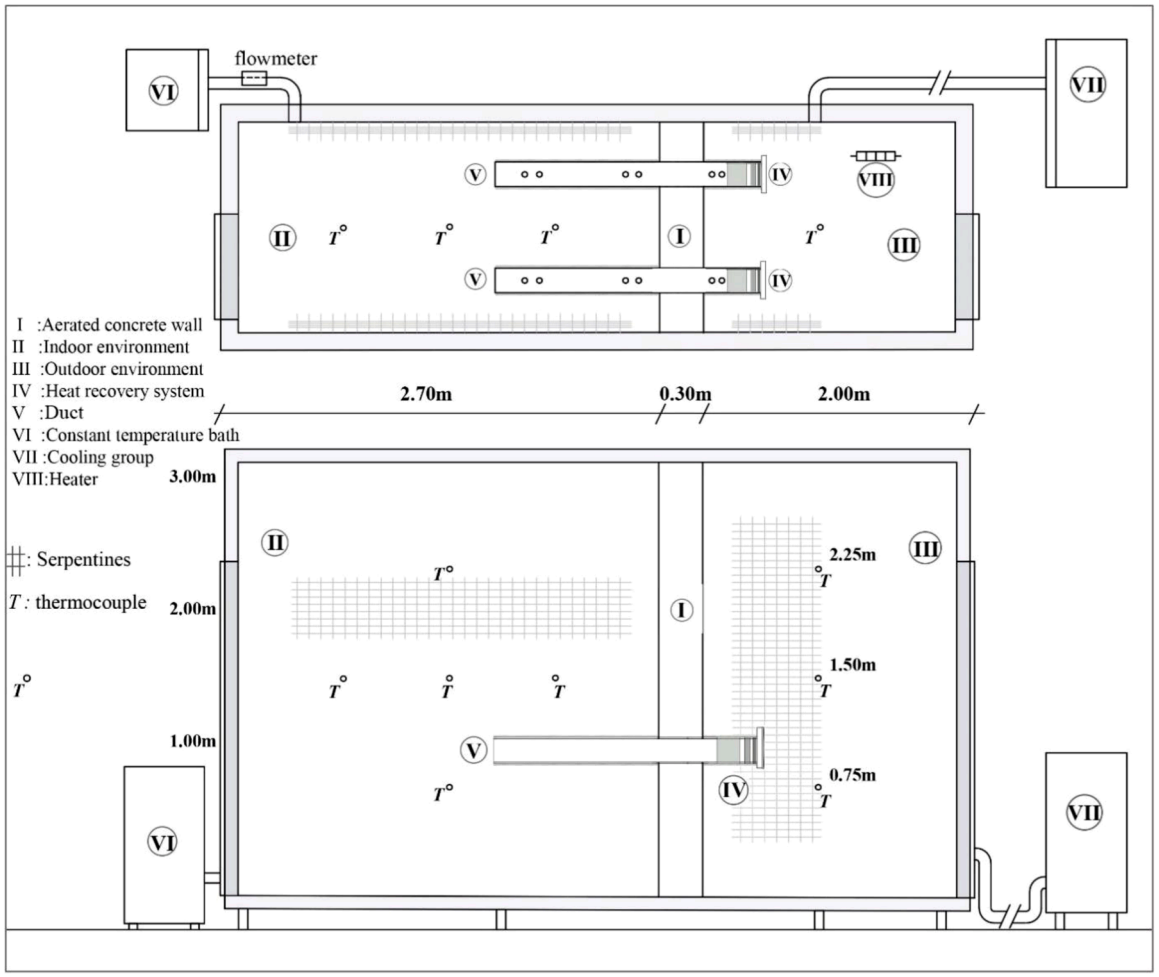

Fig. 1. Plan and section of the experimental setup (not in scale).

environment.

The experimental heat recovery systems are mounted inside the two air ducts (V) which are thermally insulated as shown in Fig. 1. The ducts are integrated with the aerated concrete wall that separates the indoor and outdoor environments. The Duct-1 and Duct-2 in Fig. 3 are placed one meter above the ground and have a cross-sectional area of 0.175 m × 0.175 m. The prototypes work in opposite directions simultaneously; thus, the air inside the ducts flow in opposing directions (in exhaust and supply modes) to minimize the pressure imbalances in the rooms that represent indoor and outdoor environments.

2.2. Experimental procedure

The experimental procedure is divided into three processes which are the preparation process, the data collection process and analyze and interpret the data process.

(1) The preparation process reaches and maintains the representative temperature conditions for the inlet and outlet sections of two HRV systems, which are closed during this period, by controlling the temperature of the indoor (22 ± 1 °C) and outdoor (35 ± 1 °C) room. Indoor and outdoor temperature values were chosen based on the indoor thermal comfort condition [29], and the average of maximum temperature measurements from Turkish State Meteorological Service between 1991 and 2020 for Izmir Turkey [30].
(2) After adjusting the system, two HRV units are used alternatively in exhaust/supply modes in periodic cycles. The thermal energy stored by the units is monitored during these periodic cycles. Throughout the experiments, indoor and outdoor temperatures, temperatures at the inlet and outlet sections of the HRV units, temperature changes in the HRV units, air velocity at the ducts where HRV units integrated, as well as the pressure differences between indoor and outdoor environments and between inlet and outlet sections of the HRV units are measured (Table 1). These experimental data measured by the instruments (mentioned in Table 1) are recorded with a datalogger in time steps of 5 s during the experiments.
(3) The reliability of the test results is determined by the uncertainty analysis given in the following section. Using the measurement results, the thermal energy storage capacity of HRV systems is calculated for different operating times.

a) indoor b) outdoor

Fig. 3. Ducts' location in simulation rooms with temperature (red dot) and velocity (blue dot) measurement points. (For interpretation of the references to color in this figure legend, the reader is referred to the web version of this article).

Table 1
Information of test instruments.

Test parameters	Test instruments	Test instrument places	Number of the test instruments
Temperature	*T*-type thermocouples	Indoor and outdoor environments	5 for indoor 3 for outdoor
		Inlet and outlet sections of the HRV units	3 for both sections (twice for Duct 1 and 2)
		Inside the tubes of HRV units	8 (twice for Duct 1 and 2)
Air velocity	Blitz Sens VS-C2-1-A Air velocity transmitter	Inlet and outlet sections of the ducts	1 (twice for Duct 1 and 2)
Differential pressure	HK Instruments DPT-R8 Analog manometer	Indoor and outdoor environments	1 instrument from 2 points for differential analysis
		Inlet and outlet sections of the HRV units	1 instrument from 2 points for differential analysis

Thermocouples within the ducts monitor the temperature variations of air and the PCM in the tubes. The melting and solidification processes of the PCM are observed with temperature measurements from many points, as detailed in the following section. Thermocouples also located at the inlet and outlet constantly monitor temperature changes of the airflow inside the ducts, and a datalogger records these measurements. The duct section and measurement points are given in Fig. 4. Two air velocity transmitters which are shown in Figs. 3a and 4, placed in the room that simulates the indoor environment measures air velocities in both ducts. Moreover, a differential pressure meter placed before and after the energy storage units records pressure drops for the exhaust and supply conditions of the units (Fig. 4). In the exhaust mode, flow is laminar and hydrodynamically fully developed close to the outlet, therefore, air velocity is measured close to the outlet from different points at the cross-section of the ducts. Meanwhile, in supply mode, the velocity measurement is taken from the specified point. Beside, a thermocouple near the outlet of the duct measures the air temperature for calculating the mass flow rate of the air considering the density variation with temperature.

The working principle of a DVS relies on the temperature differences between indoor and outdoor environments. In this study, a novel recuperative wall integrated HRV system with LHTES is developed and the improvement of the thermal energy storage performance using PCM as well as the system's pressure drop during ventilation are evaluated by conducting a full-scale experimental study for this tube bundle prototype.

At the start of each experiment, for all charging and discharging experiments, indoor and outdoor environment temperatures were monitored until the system reaches steady-state conditions while the inlet and outlet sections of the ducts were sealed with covers. A thermostat-controlled electric heater was used to stabilize the outdoor environment temperature. When the desired temperature was reached, the duct covers were opened, and the experiments started. During the experiments, two systems worked in synchrony. While one system exhausted air from the inside which took place as the discharging process for the PCM, the other one supplied fresh air from the outside which was the charging process for the PCM. The RT27 (paraffin that changes phase at 27 °C) PCM [31] was placed in the prototype. The solidification and melting process of PCM in the tube bundle were monitored during discharging and charging cycles with temperature measurements. During the experiments, temperature, flow rate, and pressure were measured utilizing the data acquisition system at 5 s intervals.

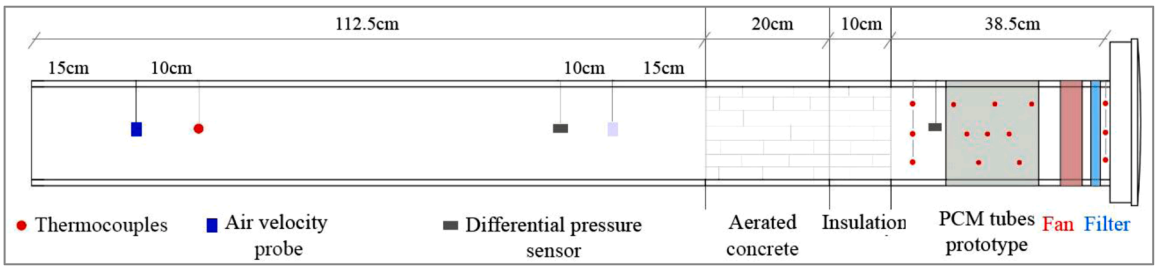

Fig. 4. Duct setup and measurement points (not to scale). (For interpretation of the references to color in this figure, the reader is referred to the web version of this article).

2.2.1. Measurement methods

For calculating and expressing the variation of the experimental setup, ambient, air velocity, pressure drop, and temperature measurements play a decisive role in significantly determining flow rates, pressure differences, and temperature changes.

The air velocity in the ducts is measured by Blitz Sens VS-C2-1-A (measurement range 0,1 m/s) air velocity transmitter [32]. First, velocity measurements were taken along the duct cross-section for exhaust and supply from 16 different points as given in Table 2, then the average velocity values in the duct sections were calculated to determine the mean airflow rates. In Duct 1, the average velocities for supply and exhaust air are 0.344 m/s and 0.282 m/s, respectively. The points that provided the nearest values to the calculated average velocity values were selected to represent the average velocity (marked in Table 2) and the following velocity measurements were taken from these points during experimental studies to determine the mean velocity, volumetric flow rate, and mass flow rate.

In the experimental setup, the differential pressure measurement was monitored with an analog manometer from two points. Two separate measurements were taken to measure the pressure difference between the indoor and outdoor environments, and the pressure difference between the systems on the two ducts with fans working in exhaust and supply modes. Fig. 5 shows the cases when the fan is working in exhaust and supply mode for cycles of 15 min, 20 min, and 30 min. While Duct 2 is operating in the exhaust mode, Duct 1 is in supply mode. When the system runs from the indoor to the outdoor environment, the fan produces an average pressure difference of 8.20 Pa for 15 min, 8.07 Pa for 20 min, and 8.02 Pa for 30 min. During the airflow from the outdoor environment to the indoor environment, the pressure difference occurring between two fans for 15 min, 20 min, and 30 min is 9.74 Pa, 9.78 Pa, and 9.57 Pa, respectively.

Koper et al. [33] measured airflow rates for different pressure drops namely 0, 4, and 7 Pa by using a single room decentralized heat recovery unit in winter conditions. For 7 Pa, the volume flow rate was 22 m^3/h in supply mode and 6 m^3/h in exhaust mode. In the study of Zemitis et al. [34], a regenerative heat exchanger effectiveness was calculated experimentally. The results showed that for a 10 Pa differential pressure, deviations in the amount of fresh air can range from 30% to 100% for the nominal flow rate of 30 m^3/h. Regarding these references, for the current experimental setup, the average pressure loss in this system is approximately 10 Pa (Fig. 5) and the volume flow rate is 28 m^3/h in supply mode and 22 m^3/h in exhaust mode. So, the fan performances of the current study were quite better than the other studies [33,34] for the same and similar pressure drops.

In experimental studies, the critical measurement for the LHTES system is the determination of the solid and liquid phases [35]. The temperature measurements of the medium are used for monitoring the melting and solidification process. The positions of thermocouples inside the test rooms representing indoors and outdoors are shown in Fig. 1. The number and location of thermocouples are as follows; one thermocouple measures the laboratory temperature, in which the experimental setup is placed, five thermocouples provide indoor environment temperature values, and three thermocouples represent outdoor environment temperature. In the indoor environment, one thermocouple is placed at the midpoint of the two-duct exit sections to measure the air temperature inside the duct for the determination of the air density. In the outdoor environment, three thermocouples measure the temperature of the system inlet in front of the filter for each duct, and three thermocouples measure the temperature of the system outlet (Fig. 4).

The tube bundle has 10 rows, and eight thermocouples are placed in the tube bundle prototype. Their placement is shown in Fig. 6. The selected tubes with a thermocouple inside are colored. These color codes are also used in the following section numbered 3, Results and Discussion. In addition, the arrangement of the thermocouples in Fig. 6 is shown with a 3D top view. These locations are selected to show the average temperature gradient in the PCM.

Calibration is important to determine the deviation of the indicator

Table 2
Duct 1 fan exhaust and supply velocity measurement results in m/s.

iv. iii. ii. i.		iv. Column	iii. Column	ii. Column	i. Column	Avg.
Supply	1. Line	0.270	0.341	0.320	0.350	0.344
	2. Line	0.306	0.345	0.371	0.403	
	3. Line	0.280	0.380	0.38	0.415	
	4. Line	0.271	0.300	0.35	0.370	
Exhaust	1. Line	0.390	0.252	0.199	0.242	0.282
	2. Line	0.395	0.251	0.225	0.278	
	3. Line	0.306	0.225	0.282	0.281	
	4. Line	0.270	0.281	0.283	0.347	

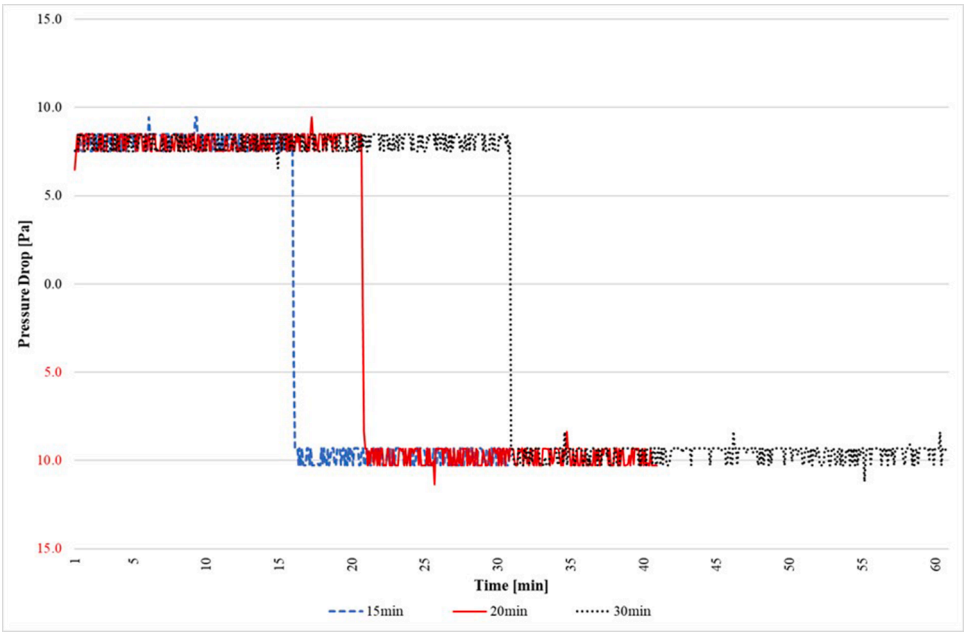

Fig. 5. The pressure difference at the inlet and outlet of the systems while the fan operates in exhaust and supply modes for three different running times.

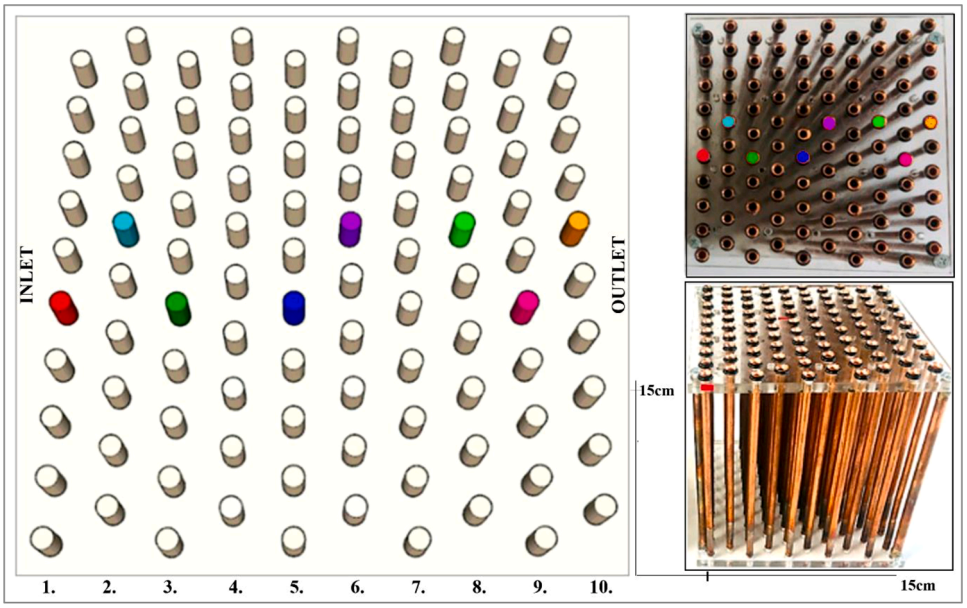

Fig. 6. Thermocouple placement inside the prototype of the decentralized HRV system with PCM.

of a measuring device from the actual value during measurement. Thermocouples were calibrated in the Chamber of Mechanical Engineers Calibration Laboratory and Metrology Training Center in İzmir, Turkey. Also, differential pressure measurement systems were self-calibrated in a case, where the pressure values were measured, and there was no pressure-generating effect; thus, the pressure values were the same in the two openings of the device. The air velocity measuring probe was calibrated by a comparison method, in which the reference sensor and the test instrument were placed in a wind tunnel test section.

In this study, uncertainties were calculated using the methodology described by Holman [36]. Air velocity measurement uncertainty during the experiments was calculated by using the manufacturer's catalog values as ~5.94% by interpolation and the uncertainty of the mass flow rate of air was calculated as ~6.27%. The total uncertainty value of the thermocouples also took the uncertainty of the devices used into consideration during the process of calibration. The overall heat transfer rate uncertainty value was ~6.35%, depending on the parameters of mass flow rate, specific heat, and temperature uncertainties.

2.2.2. *Usage of phase change material*

The most common PCMs are paraffin and salt hydrates. In this experimental study, RT27 which is paraffin that changes phase at around 27 ℃ was placed in copper tubes in liquid form. The tube bundle consists of 100 copper staggered tubes filled with PCM at the direction of the airflow. The height of one tube is 15 cm, and its outer diameter is 4.76 mm. Liquid PCM was poured into the tubes having 0.3 mm wall thickness (see Fig. 6). The tube arrangement in the bundle is designed as 1.4 cm for the transverse pitch and 1.4 cm for the longitudinal pitch. The diagonal pitch between tube centers is measured as 1.565 cm in the prototype.

The inner volume of a tube is 2.04 cm^3 and the total empty weight of the tube bundle is 906 g. When the copper tube bundle is filled with liquid PCM, it weighs 1065 g and 1062 g when the PCM solidifies due to the difference in solid-liquid density. Therefore, on average, 1.6 g of RT27 PCM [31] can be added into a tube. The physical properties of the air and copper depended on temperature, are chosen in the reference numbered [37]. On the other hand, studies numbered [38,39] are taken as the reference for the physical properties of PCM given in Table 3.

3. Results and discussion

The prototype decentralized HRV system stores latent heat thermal energy with the tube bundle containing PCM. In the context of this study, the thermal energy storage performance of the prototype is evaluated by experiments. During the experiments, while one system exhausts air from the inside, the other one supplies fresh air from the outside. However, the exhaust and supply flow of the axial fans in the heat recovery system are different from each other. Therefore, in this study, a new fan characteristic was obtained by making measurements at the fabrication speed settings. This characteristic shows that the fan operates exhaust and supply modes with 47% efficiency during the experiments [17].

3.1. Charging and discharging experiments

The experiments were conducted for the two DVS tube bundle prototypes with PCM that operate simultaneously. At the start of each experiment, the duct and the indoor environment were monitored until the system reaches steady-state conditions. After that, two HRV units installed at two ducts were used alternatively in the exhaust and supply modes in a certain periodic cycle to achieve charge and discharge conditions for the thermal energy storage of the units. Experiments continued for 15 min, 20 min, and 30 min cycles. For the simulation of summer conditions, the indoor environment temperature is maintained at around 22 ℃, and the outdoor environment is kept at approximately 35 ℃.

Temperature gradients in the tubes in the two ducts depend on the outdoor and indoor environment temperatures, as can be seen in Figs. 7–9. For the figures below (Figs. 7–9), D1 represents Duct 1 and D2 represents Duct 2. The placement of the thermocouples is coded by the number of rows in which they are located to represent the temperature individually. Duct inlet and outlet temperatures are specified as DTin and DTout, respectively. In addition, the phase change at 27 °C for PCM is indicated in all figures. In addition, all graphs contain direction indicators. These direction indicators represent the characterization test results for supply (inlet to outlet) and exhaust (outlet to inlet) of ducts. Meanwhile, Tinside and Toutside are indoor temperature and outdoor temperature, respectively.

The experiment in Figs. 7–9 is for the simulated summer conditions. Temperature changes when both units run simultaneously for Duct 1 (D1) and Duct 2 (D2). Thereby, the charging and discharging of the PCM can be monitored by following the temperature change in the thermocouples. The system operates for 15 min in one direction then, afterward it operates in the opposite direction for another 15 min (Fig. 7).

Duct 1 first takes supply air from the outside, and the PCM melts between 26 and 28 ℃. Later, when the system operates in the reverse direction, the solidification process begins (Fig. 7-D1). Temperature fluctuations occur in the outdoor environment due to the thermostat of the experimental setup. When the ambient temperature rises above or sinks below ±1#x00A0;°C, the thermostat activates and either stops or starts the heating system. Since the outdoor environment has a smaller volume, heat losses have a higher impact and cause faster cool down.

Thus, the fluctuation in the outdoor environment occurs mainly due to the thermostat-controlled heater. As seen in Fig. 7, when the systems in Ducts 1 and 2 are operated for 15 min, the PCMs in the temperature trend inside the tubes of the first three rows do not reach 27 °C, thus they are not fully melted. The other measured rows have temperatures higher than 27 °C, which shows that the PCMs are melting, and the fastest melting tube rows are the 8th and 10th. Duct 1 and Duct 2 work in opposite directions. Duct 2 is in the exhaust while Duct 1 is in the supply. In Duct 2, the fastest solidifying tube row is the PCMs inside the first two tubes. So, this figure shows that there is not enough time to stabilize the temperature distribution of the PCMs inside all the tubes. For this reason, the system must operate for a while for the PCM to melt or solidify. Hence, the system was operated for different operation times, and Figs. 8 and 9 give the results.

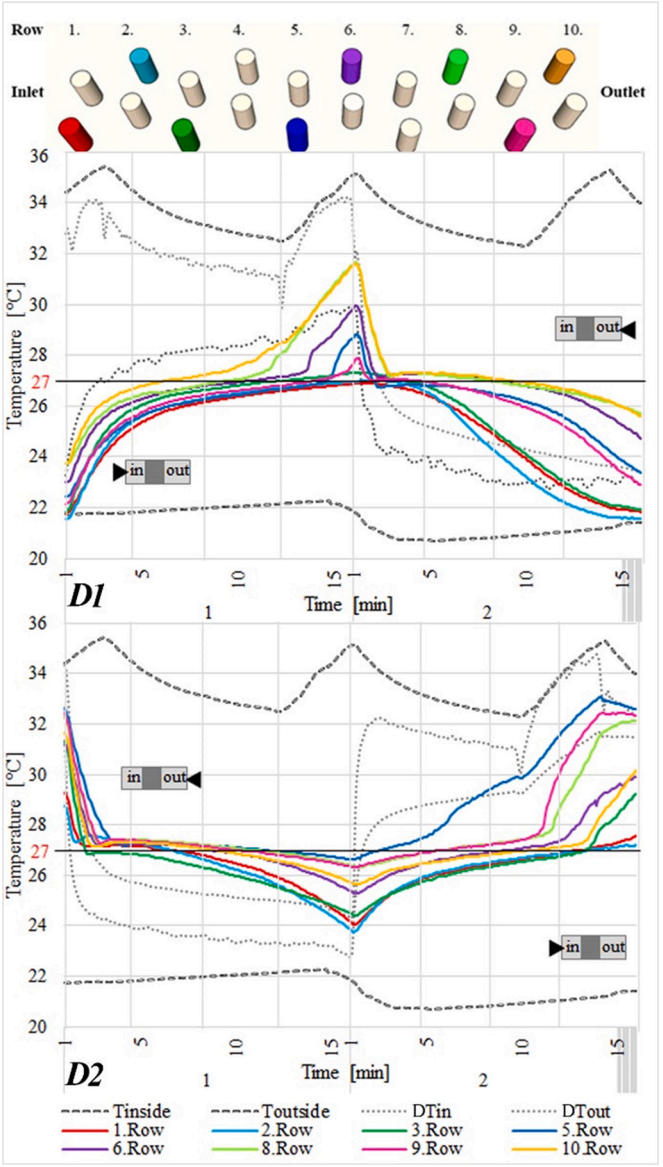

Fig. 7. Heat recovery system operation for 30 min, with 15 min cycles in summer conditions for Duct 1 (D1) and Duct 2 (D2).

Table 3
Physical properties of RT27 [31,38,39].

Properties	Values for RT27
Density, solid phase (15℃)	880 kg/m^3
Density, liquid phase (40℃)	760 kg/m^3
Specific heat	2.4 kJ/kg·K
Latent heat	184 kJ/kg
Thermal conductivity	0.2 W/m·K

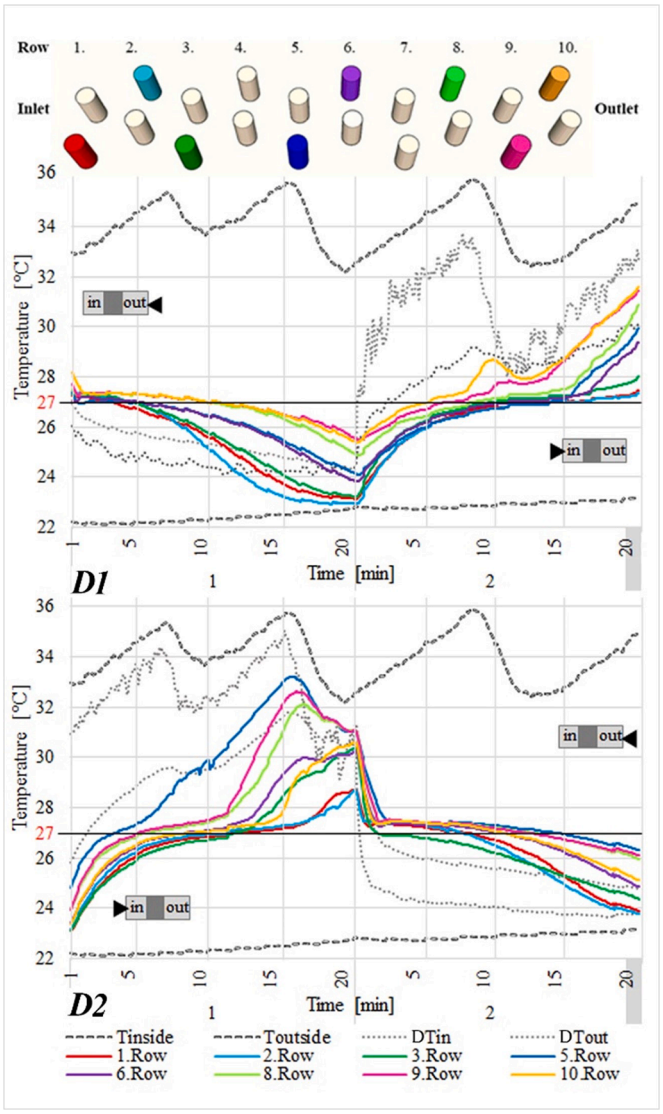

Fig. 8. Heat recovery system operating for 40 min with 20 min cycles in summer conditions for Duct 1 (D1) and Duct 2 (D2).

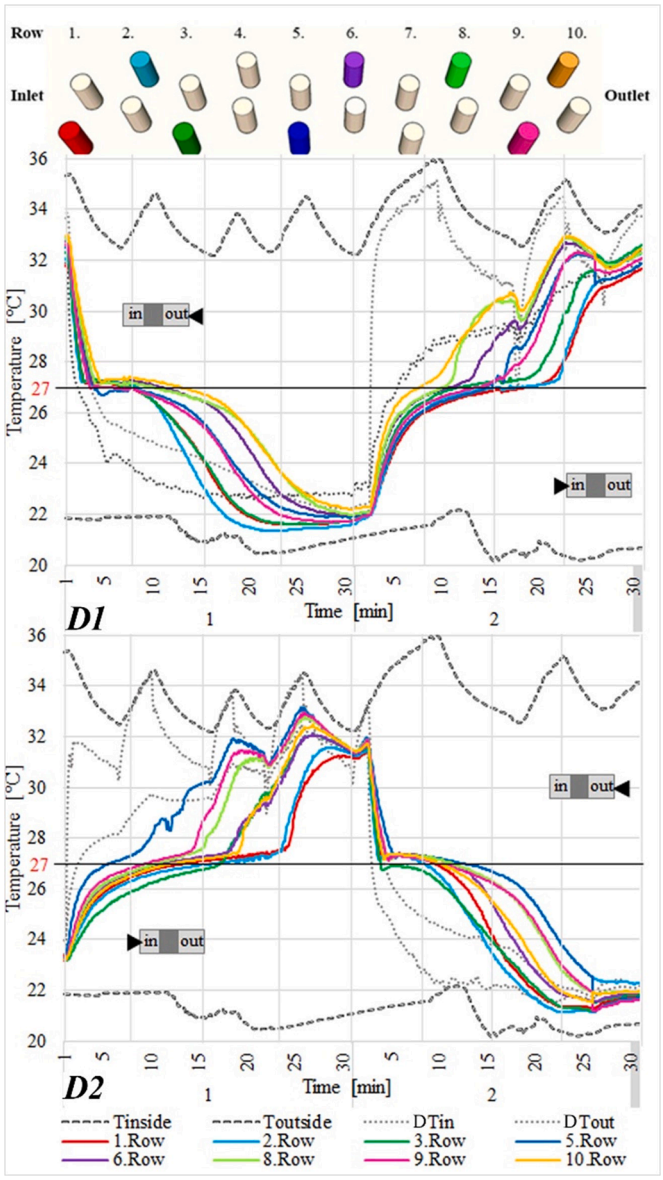

Fig. 9. Heat recovery system operating for 60 min with 30 min cycles in summer conditions for Duct (D1) and Duct 2 (D2).

Fig. 8 shows the results of 20 min of operation for summer. At the beginning of the experiment, while the fan in Duct 1 supplies air, the fan in Duct 2 exhausts air from the indoor environment. The average indoor temperature is 22 ℃, and the outdoor temperature is around 35 ℃. While one cycle duration is 40 min, Fig. 8 shows two 20 min exhaust and supply modes for D1 and D2. The figure shows that the melting and solidification process sufficiently occurs in the PCM tubes. Looking at the rows one by one, the ones with the lowest temperatures in exhaust mode are the first two rows in D1. In the supply mode, in D2, the fastest melting row is the 5th and 9th. Then it is 8th, 10th, 6th, 3rd, 1st, and 2nd, respectively. Moreover, when the system operates for 20 min, the temperature increases inside the tube bundle, and the melting and solidification process of the PCM performs better than the 15 min cycle presented in Fig. 7.

Fig. 9 gives the results of operation for 30 min of exhaust and 30 min of supply modes. Thus, the cycle is 60 min in total. The indoor temperature value is 21 ± 1 °C on average, while the outdoor temperature is around 33 ℃. As can be seen, PCM completely melts in Duct 2 and completely solidifies in Duct 1 in 30 min. Then, the temperatures of the thermocouples increase. This indicates that sensible heat storage follows LHTES. Thus, the temperatures of these thermocouples get very close to the indoor or outdoor environment when the system operates for 30 min.

When Duct 1 is in exhaust mode, the first two rows are solidifying first. And then 3rd, 9th, 5th, 6th, 8th, and 10th are solidifying, respectively. While Duct 2 is operating in supply mode, the first row of melting tubes is the 5th and 9th row. Then the rows of tubes 8th, 6th, 3rd, 10th, 1st, and 2nd, are melted, respectively.

Fig. 10 shows the melting process of the PCM inside the tubes while working in the supply mode. This color chart represents the temperatures measured in the tubes from blue to red. Red is the 35 °C which is the row of tubes with the highest temperature, while blue represents 27 °C is the row of tubes that have not completely melted which is the mushy zone. When the system operates for 15 min, the first three rows are not fully melted. And in all operation time, the last three rows have the highest temperature when system operating supply mode.

3.2. Data reduction

Table 4 shows the results of the tube bundle HRV system with PCM obtained from experimental data and calculations. In sensible heat storage systems, the variables that determine the amount of energy

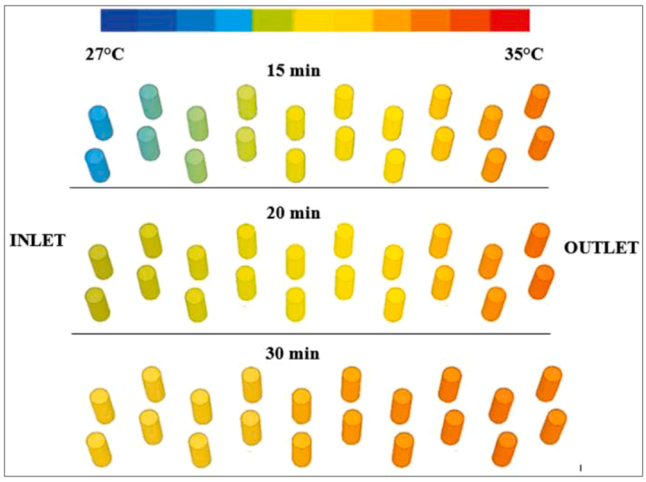

Fig. 10. Temperature distribution for rows at the end of an operation cycle in supply mode.

stored are the amount of material used, the specific heat of the material, and the temperature change that takes place during the heat storage. The amount of heat stored in/released from the PCM to the air is calculated by using Eq. (1);

$$Q = \dot{m} c_p \Delta T \Delta t \tag{1}$$

where $\dot{m}$ is the mass flow rate of air (kg/s), c_p is the air specific heat capacity (J/kg°C), ΔT is the temperature change of air (°C), and Δt is the running time period (s). The results of the experiments are presented in Table 4. The air energy change is obtained according to the weighted averages of three thermocouples (Tin) placed before the filter in the unit, and the average of the three thermocouples (Tout) placed after the prototype and air velocity data measurements during specified time steps.

The PCM, RT27 can store latent heat and is used in the prototype to add more energy storage capacity according to the temperature and phase changes in the material. So, when calculating the internal energy change in the PCM during the experiment, both of the physical processes of heat storage; sensible heat and latent heat, occur and need interpretation. Sensible heat is related to the temperature change of a substance, while latent heat depends on the phase change of the material, namely liquid to solid or solid to liquid phases in this study. Since phase change enthalpy is used to overcome the molecular attraction of particles, it has many times more energy storage capacity than sensible heat [40].

Furthermore, air energy changes shown in Table 4 are used to investigate the performance of the heat recovery system. The storage rate per unit time is an important parameter for evaluation rather than the actual running period of the system. According to Table 4, when the system operates for 20 min, the system performs better than 15 and 30 min. Also, when looking at the calculation of the average storage rate per unit time, the best performance can be seen by operating the system for 20 min. The thermal energy stored in the system from the previous cycle or waiting for the time variations between the cycles are the reasons for the difference in supply and exhaust values for heat transfer rates.

The best possible thermal efficiency cannot always be achieved due to experimental uncertainties and errors, as well as poor setup or breakdown during operation. To obtain the efficiency of the unit, it is calculated according to the following procedures described in European Standard EN 13,141-8:2014 for non-ducted units to measure temperature ratio on the supply air side [41]. The heat recovery efficiency used in the calculations is given for the supply air side temperature ratio by using Eq. (2):

$$\eta = \frac{1}{t_{cycle}} \left[\int_{t}^{t+\Delta t} \left(\frac{T_{21} - T_{22}}{T_{21} - T_{11}} \right) dt \right] \times 100 \tag{2}$$

where;

T_{21} = supply inlet temperature (°C)
T_{22} = supply outlet temperature (°C)
T_{11} = inside temperature (°C)

η defines the efficiency of the decentralized heat recovery prototype for different working conditions. The temperature measurements are recorded at 5-second intervals (Δt), and the efficiencies are calculated by using specified operating time cycles which are 15 min, 20 min, and 30 min represented by t_{cycle}. The supply efficiency results calculated according to Eq. (2) are 51.6% for 15 min, 54.9% for 20 min, and 46.7% for 30 min. And exhaust efficiency results are 23.3%, 29.8% and 24.6%, respectively.

Another consideration for designing such a wall-embedded system included a decentralized heat recovery ventilation is inside and outside pressure difference induced by the wind and stack effects. Although the stack effect is already considered in this current study (pressure drop values are different for the exhaust and supply modes in Fig. 5 because of the stack effect), the wind effect is not included because of the laboratory experiment conditions. But, in the real working condition of these wall-embedded systems, the wind effect should be considered and the system in the wall is installed avoiding prevailing wind direction. According to Merzkirch et al. [14], the heat recovery efficiency can be reduced 8–22% because of the wind and/or stack effect. The heat exchanger unit's efficiency is dependent on the pressure difference, if the pressure differences are around 10 Pa to 20 Pa, the efficiency is changing between 20 and 50%. Filis et al. [42] validated an average of 62% sensible heat recovery efficiency at 5.2 Pa negative pressure difference in their simulations. Although mentioned studies [14,17,42] about the decentralized heat recovery ventilation system included sensible energy storage unit, gave the better performances, the present study included latent energy storage unit provided an efficiency between 25 to 55% under the specified laboratory condition. This latent energy storage system should be improved considering different tube heat exchanger designs for better efficiency of the system which is another study subject for future studies.

4. Conclusions

A novel latent HRV system, which aims to increase the energy performance of the buildings, while taking fresh air to the interior, is experimentally investigated under different operating conditions. In the

Table 4
Air energy change of the latent HRV prototype.

Time [min]	Direction [*in*: inlet, *out*: outlet]	D2-T_{in_Avg} [°C]	D2-T_{out_Avg} [°C]	D2-Air_Vel [m/s]	Std. Dev. of Vel.	Energy Change [kJ]	Avg. Storage Rate (Watt)
15	*in* to *out*	32.10	29.85	0.35	0.025	16.12	17.9
	out to *in*	26.02	24.29	0.30	0.010	14.68	16.3
20	*in* to *out*	30.46	28.34	0.32	0.056	27.24	22.7
	out to *in*	25.56	23.97	0.29	0.012	22.13	18.4
30	*in* to *out*	32.01	30.05	0.35	0.025	34.12	19.0
	out to *in*	24.17	23.39	0.32	0.027	19.88	11.0

experimental test chamber, two ducts are integrated into an insulated wall representing an exterior wall that separates the indoor and outdoor environments. Units installed in these ducts operate simultaneously to prevent pressure imbalances. According to the experiments, the melting/solidifying results show that 20 min operation time gives the best thermal performance for maintaining a comfortable indoor temperature with the least energy consumption according to the storage rate. Meanwhile, the supply mode efficiency result is an average of 50% and exhaust mode efficiency is 25% for simulated summer conditions.

Experimental studies all have some limitations. In this study, a more accurate temperature distribution in the tube could be observed by taking more measurements while the system is working. Different phase change materials could be also investigated experimentally under different indoor and outdoor conditions; especially winter conditions could be studied as future studies. Another issue that needs reconsideration is the fan. Although the fans serve to exhaust and supply functions at the same time, the exhaust direction operates with a lower flow rate compared to the supply direction. Therefore, due to the high flow rate, there is a more homogeneous distribution in the prototype during the flow of fresh air from the outdoor environment to the indoor environment than the air transfer from the indoor environment. For these two operations, a pitch control fan or two separate fans can provide more effective ventilation performance. This system can also contribute to a healthy indoor environment by meeting the fresh air requirement that is an important element of IAQ. Therefore, changes in the levels of IAQ variables including, temperature, relative humidity, and carbon dioxide levels must be experimentally investigated.

The prototype adds LHTES into ventilation systems by the integration of PCMs. Hence, it is an alternative to the ceramic systems in the market under different climatic conditions. Yet, more research and development are necessary before the prototype can enter the market. According to the experimental results, it is necessary to examine the environmental characteristics of the building on which the system will be used depending on the months and seasons on a micro-climatic scale for the selection of suitable PCMs in different temperature ranges. This study became a possible starting point for further studies to create design guidelines for DVSs with latent heat, where the experimental setup will be modeled, analyzed, and compared with the experimental results. Therefore, creating a valid simulation model, and conducting the necessary parametric investigation for different seasons, months, and choices of PCM to turn the prototype into a product is the authors' next study priority.

CRediT authorship contribution statement

Tugce Pekdogan: Visualization, Formal analysis, Writing – original draft, Writing – review & editing, Data curation. **Ayça Tokuç:** Methodology, Conceptualization, Investigation, Writing – review & editing. **Mehmet Akif Ezan:** Methodology, Conceptualization, Investigation, Writing – review & editing. **Tahsin Başaran:** Conceptualization, Supervision, Methodology, Writing – review & editing, Project administration.

Declaration of Competing Interest

The authors declare that they have no known competing financial interests or personal relationships that could have appeared to influence the work reported in this paper.

Acknowledgment

This work was supported by the Scientific and Technological Research Council of Turkey (TUBITAK) Foundation under grant number 217M366.

References

[1] US Environmental Protection Agency (EPA). Report to Congress on indoor air quality, volume II: assessment and control of indoor air pollution., Technical Report EPA/400/1-89/001C, 1989.
[2] R. Afshari, Indoor air quality and severity of COVID-19: where communicable and non-communicable preventive measures meet, Asia Pac. J. Med. Toxicol. 9 (2020) 1–2, https://doi.org/10.22038/APJMT.2020.15312.
[3] G. Köktürk, A. Tokuç, Vision for wind energy with a smart grid in Izmir, Renew. Sustain. Energy Rev. (2017), https://doi.org/10.1016/j.rser.2017.01.147.
[4] S.S. Chandel, T. Agarwal, Review of cooling techniques using phase change materials for enhancing efficiency of photovoltaic power systems, Renew. Sustain. Energy Rev. (2017), https://doi.org/10.1016/j.rser.2017.02.001.
[5] P.M. Cuce, S. Riffat, A comprehensive review of heat recovery systems for building applications, Renew. Sustain. Energy Rev. 47 (2015) 665–682, https://doi.org/10.1016/j.rser.2015.03.087.
[6] L. Shao, S.B. Riffat, G. Gan, Heat recovery with low pressure loss for natural ventilation, Energy Build. 28 (1998), https://doi.org/10.1016/s0378-7788(98)00016-4.
[7] A. Mardiana-Idayu, S.B. Riffat, An experimental study on the performance of enthalpy recovery system for building applications, Energy Build. (2011), https://doi.org/10.1016/j.enbuild.2011.06.009.
[8] C. Zeng, S. Liu, A. Shukla, A review on the air-to-air heat and mass exchanger technologies for building applications, Renew. Sustain. Energy Rev. 75 (2017) 753–774, https://doi.org/10.1016/j.rser.2016.11.052.
[9] P. Wallner, P. Tappler, U. Munoz, B. Damberger, A. Wanka, M. Kundi, H.P. Hutter, Health and wellbeing of occupants in highly energy efficient buildings: a field study, Int. J. Environ. Res. Public Health 14 (2017), https://doi.org/10.3390/ijerph14030314.
[10] A. Fonseca, I. Abreu, M.J. Guerreiro, C. Abreu, R. Silva, N. Barros, Indoor air quality and sustainability management-case study in three Portuguese healthcare units, Sustainability 11 (2018), https://doi.org/10.3390/su11010101.
[11] M. Verriele, C. Schoemaecker, B. Hanoune, N. Leclerc, S. Germain, V. Gaudion, N. Locoge, The MERMAID study: indoor and outdoor average pollutant concentrations in 10 low-energy school buildings in France, Indoor Air 26 (2016), https://doi.org/10.1111/ina.12258.
[12] J.S. Park, N.Y. Jee, J.W. Jeong, Effects of types of ventilation system on indoor particle concentrations in residential buildings, Indoor Air 24 (2014), https://doi.org/10.1111/ina.12117.
[13] M.K. Kim, L. Baldini, Energy analysis of a decentralized ventilation system compared with centralized ventilation systems in European climates: based on review of analyses, Energy Build. 111 (2016) 424–433, https://doi.org/10.1016/j.enbuild.2015.11.044.
[14] A. Merzkirch, S. Maas, F. Scholzen, D. Waldmann, Field tests of centralized and decentralized ventilation units in residential buildings - specific fan power, heat recovery efficiency, shortcuts and volume flow unbalances, Energy Build. (2016), https://doi.org/10.1016/j.enbuild.2015.12.008.
[15] D.W. Etheridge, M. Sandberg, Ventilation rate measurements. Building Ventilation: Theory and Measurement, John Wiley & Sons, UK, 1996.
[16] AHSRAE. ANSI/ASHRAE Standard 62.1-2019, Ventilation for Acceptable Indoor Air Quality, 2019.
[17] T. Pekdogan, A. Tokuç, M.A. Ezan, T. Başaran, Experimental investigation of a decentralized heat recovery ventilation system, J. Build. Eng. 35 (2021), https://doi.org/10.1016/j.jobe.2020.102009.
[18] M.M. Farid, A.M. Khudhair, S.A.K. Razack, S. Al-Hallaj, A review on phase change energy storage: materials and applications, Energy Convers. Manag. 45 (2004) 1597–1615, https://doi.org/10.1016/j.enconman.2003.09.015.
[19] P. Promoppatum, S.C. Yao, T. Hultz, D. Agee, Experimental and numerical investigation of the cross-flow PCM heat exchanger for the energy saving of building HVAC, Energy Build. 138 (2017) 468–478, https://doi.org/10.1016/j.enbuild.2016.12.043.
[20] N. Soares, J.J. Costa, A.R. Gaspar, P. Santos, Review of passive PCM latent heat thermal energy storage systems towards buildings' energy efficiency, Energy Build. 59 (2013) 82–103, https://doi.org/10.1016/j.enbuild.2012.12.042.
[21] N. Stathopoulos, M. El Mankibi, R. Issoglio, P. Michel, F. Haghighat, Air-PCM heat exchanger for peak load management: experimental and simulation, Sol. Energy 132 (2016), https://doi.org/10.1016/j.solener.2016.03.030.
[22] Y. Hu, P.K. Heiselberg, H. Johra, R. Guo, Experimental and numerical study of a PCM solar air heat exchanger and its ventilation preheating effectiveness, Renew. Energy 145 (2020) 106–115, https://doi.org/10.1016/j.renene.2019.05.115.
[23] S. Van Berkel, K.D. Pressnail, M.F. Touchie, Residential ventilation: a review of established systems and a preliminary laboratory investigation of an innovative fine wire heat recovery ventilator, in: Proceedings of the 14th Canadian Conference on Building Science and Technology, 2014, pp. 381–391.
[24] A. Mikola, R. Simson, J. Kurnitski, The impact of air pressure conditions on the performance of single room ventilation units in multi-story buildings, Energies 12 (2019), https://doi.org/10.3390/en12132633.
[25] T. Inan, T. Başaran, M.A. Ezan, Experimental and numerical investigation of natural convection in a double skin facade, Appl. Therm. Eng. (2016), https://doi.org/10.1016/j.applthermaleng.2016.06.124.
[26] T. Başaran, T. İnan, Experimental investigation of the pressure loss through a double skin facade by using perforated plates, Energy Build. (2016), https://doi.org/10.1016/j.enbuild.2016.10.020.
[27] T. Inan, T. Basaran, A. Erek, Experimental and numerical investigation of forced convection in a double skin façade, Energies 10 (2017) 1–15. 10.3390/en10091364.

[28] T. Inan, T. Basaran, Experimental and numerical investigation of forced convection in a double skin façade by using nodal network approach for Istanbul, Sol. Energy 183 (2019), https://doi.org/10.1016/j.solener.2019.03.030.
[29] ANSI/ASHRAE Standard 55R Thermal Environmental Conditions for Human Occupancy, American Society of Heating, Refrigerating and Air-Conditioning Engineers Inc., Atlanta, 2004.
[30] Republic of Turkey General Directorate of State Meteorological Service. https://www.mgm.gov.tr/veridegerlendirme/il-ve-ilceler-istatistik.aspx?k=H (accessed 18 September 2021).
[31] Rubitherm Technologies GmbH. Rubitherm GmbH. Rubitherm GmbH (2020).
[32] Nielsen P.Y. 12 experimental technıques 2001. 10.1016/B978-012289676-7/50015-1.
[33] P. Koper, A. Palmowska, A. Myszkowska, Research of single room decentralized heat recovery unit, Archit. Civ. Eng. Environ. 12 (2020) 109–114, https://doi.org/10.21307/acee-2019-056.
[34] J. Zemitis, A. Borodinecs, A. Geikins, T. Kalamees, K. Kuusk, Ventilation system design in three European geo cluster, Energy Procedia 96 (2016) 285–293, https://doi.org/10.1016/j.egypro.2016.09.151.
[35] M.A. Ezan, M. Ozdogan, A. Erek, Experimental study on charging and discharging periods of water in a latent heat storage unit, Int. J. Therm. Sci. 50 (2011), https://doi.org/10.1016/j.ijthermalsci.2011.06.010.
[36] Holman J.P. Experimental methods for engineers. (2012).
[37] ASHRAE, ANSI/ASHRAE Handbook Fundamentals, ASHRAE, 2017. Materials.
[38] A. Tokuç, T. Başaran, S.C. Yesügey, An experimental and numerical investigation on the use of phase change materials in building elements: the case of a flat roof in Istanbul, Energy Build. 102 (2015), https://doi.org/10.1016/j.enbuild.2015.04.039.
[39] B. Durakovic, M. Torlak, Experimental and numerical study of a PCM window model as a thermal energy storage unit, Int. J. Low-Carbon Technol. (2016), https://doi.org/10.1093/ijlct/ctw024.
[40] I. Dincer, M.A Ezan, Heat Storage: A Unique Solution for Energy Systems, Springer, 2018.
[41] EN 13141-8:2014. Ventilation for buildings. Performance testing of components/products for residential ventilation. Performance testing of un-ducted mechanical supply and exhaust ventilation units (including heat recovery) for mechanical ventilation systems intended for a 2014.
[42] V. Filis, J. Kolarik, K.M. Smith, The impact of wind pressure and stack effect on the performance of room ventilation units with heat recovery, Energy Build. 234 (2021), https://doi.org/10.1016/j.enbuild.2020.110689.